Exact Poisson-Boltzmann solution for the interaction of dissimilar charge-regulating surfaces

Sven Holger Behrens[1,2,*] and Michal Borkovec[1]
[1]*Center for Advanced Materials Processing, Clarkson University, Potsdam, New York 13699-5814*
[2]*Swiss Federal Institute of Technology, ETHZ-ITO, Grabenstrasse 3, 8952 Schlieren, Switzerland*
(Received 26 May 1999)

An efficient method is proposed to calculate the electric double layer force between two flat surfaces of dissimilar composition and ionization properties. The approach is based on explicit expressions for the solution of the (nonlinear) Poisson-Boltzmann equation and allows for boundary conditions of charge regulation, i.e., chemical equilibrium of both surfaces with a bulk electrolyte at all surface separations. As an illustration, we discuss in some detail the interaction between a weakly acidic and a strongly acidic latex surface, and between an acidic (silica) surface and an amphoteric (rutile) surface. [S1063-651X(99)16511-5]

PACS number(s): 82.70.Dd, 82.65.−i, 68.45.−v

I. INTRODUCTION

Understanding and manipulating the interaction of charged colloidal surfaces has always been a central task in colloid science [1]. More recently, the accessibility of colloidal forces to direct measurements with the surface force apparatus [1–5] and the atomic force microscope [6–11] has triggered an intensified search for a quantitative theoretical description of the force profiles. Whenever the radius of curvature of the interacting surfaces is large by comparison to the decay length of the interaction, a good starting point is the consideration of two infinite parallel plates (half-spaces, to be precise). The interaction in this idealized system can easily be transformed into the one between two bodies with curved surfaces via the Derjaguin approximation [12]. An important component of the interaction is typically considered to be of purely electrostatic nature. In compliance with the classical Derjaguin-Landau-Verwey-Overbeek theory [13,14], this contribution is treated separately from the other components and is described on the basis of the Poisson-Boltzmann equation [12]. For surfaces of very high charge density, especially in the presence of multivalent ions, this treatment is known to be inadequate, because it neglects the effect of ion-ion correlations [15]. For many situations of interest, Poisson-Boltzmann predictions have been confirmed experimentally, however, and this classical approach has greatly helped to develop a conceptual understanding of charged colloidal and polymeric systems [1].

Ninham and Parsegian [16] solved the case of identical surfaces with ionizable groups in equilibrium with a bulk electrolyte solution (charge regulation), using exact expressions for the resulting interaction in terms of Jacobian elliptic functions. The charge-regulation model was then adapted to the case of amphoteric functional groups by Chan and coworkers [17,18]. A first quantitative discussion of the important case of dissimilar surfaces by Prieve and Ruckenstein [19] was based on a numerical treatment of the Poisson-Boltzmann equation.

Many studies have since been made on charge-regulating surfaces [20–38]. Yet, to our knowledge, no strategy has so far been proposed that actually generalizes the exact expressions of Ninham and Parsegian [16] to the case of dissimilar surfaces. The available quantitative treatments for such surfaces require a numerical solution of the differential equation [19–21,23,35] or involve further approximations like the linearization of the Poisson-Boltzmann equation [29,36] or the use of simplified boundary conditions such as a constant surface charge or constant surface potential [33,34]. The present work fills this gap by providing an exact solution to the problem of dissimilar, charge-regulating surfaces on the Poisson-Boltzmann level.

II. ELECTROSTATIC FORCES BETWEEN DISSIMILAR SURFACES

We consider the interaction of two infinite, homogeneously charged planar surfaces across a solution of a $z-z$ electrolyte [39]. The electrolyte between the surfaces will be imagined in equilibrium with a large solution bulk, and the electrostatic potential in the interstitial region will be assumed to satisfy the Poisson-Boltzmann equation [12]

$$\frac{d^2\Psi}{dx^2} = \kappa^2 \sinh \Psi. \tag{1}$$

Here $\Psi = e_0 z \psi/(k_B T)$ is the dimensionless electrostatic potential, ψ being the actual potential, e_0 the protonic charge, and $k_B T$ the thermal energy; x is the space coordinate normal to the surfaces, and $\kappa^{-1} = [\varepsilon \varepsilon_0 k_B T/(2e_0^2 z^2 n)]^{1/2}$ is the Debye screening length, which further depends on the electrolyte concentration n and the permittivity $\varepsilon\varepsilon_0$ of the bulk solution. The bulk will also be chosen as the point of reference for the electrostatic potential, i.e., we set $\Psi(\text{bulk}) = 0$.

Our goal is an exact and efficient evaluation method for the force per unit area between the two surfaces at any surface separation. Once this force is known, the interaction energy per unit area as well as various interaction properties of curved surfaces in the Derjaguin approximation can be obtained by straightforward integration [12,38].

No restriction concerning the boundary conditions for Eq. (1) shall be imposed at this point. In particular, we will allow the surface charge and potential to vary with the surface

*Author to whom correspondence should be addressed. Electronic address: behrenss@clarkson.edu

separation in a different way for the two surfaces, as would be expected for surface materials of different ionization characteristics.

A. A useful parametrization

First we note that the dividing pressure Π we are looking for can be written as the sum of an osmotic repulsion and an attractive Maxwell stress term; the normalized dimensionless pressure reads [12]

$$P=\frac{\Pi}{nk_BT}=2(\cosh\Psi-1)-\kappa^{-2}\left(\frac{d\Psi}{dx}\right)^2. \tag{2}$$

Note that the value of P does not depend on the position x between the surfaces at which the potential and its derivative are evaluated. Any solution $\Psi(x)$ of the Poisson-Boltzmann equation [Eq. (1)] has a curvature of the same sign as Ψ itself, i.e., it ''bends away from the x axis'' for all x. Accordingly, $\Psi(x)$ can go through zero at most once. Three cases can be distinguished: (i) $\Psi(x)$ can have a maximum or minimum at some point, which we will then choose as the point of reference where $x=0$; in this case the function $\Psi(x)$ has no zero; (ii) $\Psi(x)$ can go through zero at some point, which will now serve as the origin of the space coordinate; or (iii) the curve can reach zero asymptotically. [In this case, we will choose an arbitrary point as the origin and use an expression for $\Psi(x)$ that does not depend on this choice of origin].

Since $\Psi(x)$ is fully determined by the differential equation (1) together with the value of Ψ and $d\Psi/dx$ at one point, it is clear that $\Psi(x)$ must be symmetric in case (i) and antisymmetric in case (ii). From Eq. (2) (evaluated at $x=0$) it follows that case (i), depicted in Fig. 1(a), describes a situation of positive pressure (repulsion), whereas case (ii), illustrated in Fig. 1(b), represents a potential profile associated with negative pressure (attraction). The third case obviously represents a transition between the repulsive and the attractive case and thus corresponds to a situation of zero force.

For all of these cases, the solutions of Eq. (1) are well known [16,33]; in the present frame of reference they take a particularly simple form, which we proceed to state explicitly. Their derivation is given in the Appendix. Since every pressure corresponds to just one potential profile (or its negative), it is convenient to think of the pressure value P as a parameter of the solutions $\Psi(x)$.

1. Repulsion

In the case of positive pressures and for $\Psi<0$, $x\geqslant 0$ (other ranges follow by symmetry), the solution $\Psi(x)$ of Eq. (1) is given in terms of the potential

$$\Psi_0=\Psi(0)=\operatorname{arccosh}(1+P/2) \tag{3}$$

as

$$\Psi(x)=\Psi_0+2\ln\operatorname{cd}(u|m), \tag{4}$$

with

$$u=\frac{1}{2}e^{-\Psi_0/2}\kappa x$$

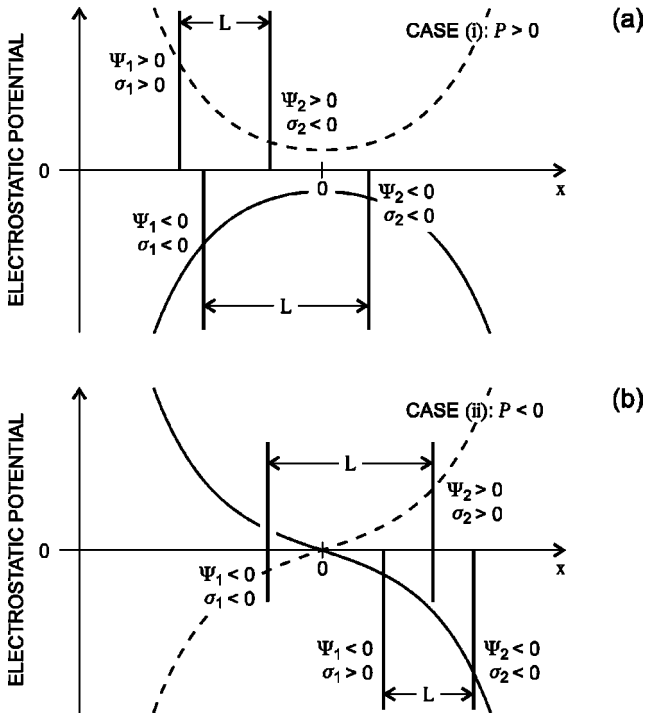

FIG. 1. The solutions $\Psi(x)$ of the Poisson-Boltzmann equation. For every nonzero value P of the dimensionless pressure [Eq. (2)] there is exactly one solution $\Psi(x)$ (and its negative). Any pair of straight lines intersecting the solution curve at the positions x_1 and x_2 can be interpreted as a pair of charged surfaces with separation distance $L=|x_1-x_2|$ interacting with the pressure P and bearing the surface potentials $\Psi_j=\Psi(x_j)$, $j=1,2$, and surface charge densities σ_1,σ_2 given by the derivative of $\Psi(x)$ in x_1 and x_2. (a) Case (i): Whenever the pressure is positive (repulsion), the solution $\Psi(x)$ qualitatively resembles a hyperbolic cosine. This is the only possible type of interaction for two surfaces with the same sign of charge [42]. (b) Case (ii): If the pressure is negative (attraction), then $\Psi(x)$ qualitatively resembles the hyperbolic sine.

and

$$m=e^{2\Psi_0},$$

where $\operatorname{cd}(u|m)$ is a Jacobian elliptic function of argument u and parameter m [40]. For future reference, we also give the derivative

$$\frac{d\Psi}{dx}=(e^{3\Psi_0/2}-e^{-\Psi_0/2})\kappa\frac{\operatorname{sn}(u|m)}{\operatorname{cn}(u|m)\operatorname{dn}(u|m)}, \tag{5}$$

where $\operatorname{sn}(u|m),\operatorname{cn}(u|m)$, and $\operatorname{dn}=\operatorname{cn}/\operatorname{cd}$ are again Jacobian elliptic functions of the argument u and parameter m given above. Efficient implementations of these functions are available from modern mathematical libraries [41].

2. Attraction

In the attractive case, the solution (for $\Psi\leqslant 0\leqslant x$) expressed in terms of the pressure

$$P=-\kappa^{-2}\left(\frac{d\Psi}{dx}\right)^2_{x=0} \tag{6}$$

reads

$$\Psi(x)=\begin{cases} -2\,\mathrm{arctanh}\left[\frac{1}{2}(-P)^{1/2}\,\mathrm{sd}(\kappa x|1+P/4)\right], & -4\leqslant P<0 \\ -2\,\mathrm{arctanh}\left[\mathrm{sn}\left(\frac{1}{2}(-P)^{1/2}\kappa x\middle|1+4/P\right)\right], & P\leqslant -4, \end{cases} \tag{7}$$

where sd=sn/dn is yet another elliptic function in standard notation [40]. Note that the solutions for pressures below and above $P=-4$ match; at this transition pressure the solution is $\Psi(x)=-2\,\mathrm{arctanh}(\sin\kappa x)$.

The derivative is

$$\frac{d\Psi}{dx}=\begin{cases} -\kappa(-P)^{1/2}/\mathrm{cn}(\kappa x|1+P/4), & -4\leqslant P<0 \\ -\kappa(-P)^{1/2}/\mathrm{cd}(\frac{1}{2}(-P)^{1/2}\kappa x|1+4/P), & P\leqslant -4, \end{cases} \tag{8}$$

with $\Psi(x)=-2\kappa/\cos\kappa x$ for $P=-4$.

3. Configuration of zero force

The situation where the charged surfaces neither repel nor attract each other ($\Pi=0$) is described by the familiar Gouy-Chapman theory for a single charged plate [12]. The decay of the potential from its surface value Ψ_1 at position x_1 is given by

$$\Psi(x)=4\,\mathrm{arctanh}[e^{-\kappa(x-x_1)}\,\tanh(\Psi_1/4)], \tag{9}$$

and the derivative reads

$$\frac{d\Psi}{dx}=-\frac{4\kappa\,\tanh(\Psi_1/4)e^{-\kappa(x-x_1)}}{1-\tanh^2(\Psi_1/4)e^{-2\kappa(x-x_1)}}=-2\kappa\sinh(\Psi/2). \tag{10}$$

B. Dissimilar surfaces

For a given potential profile $\Psi(x)$ of the type described by Eqs. (4)–(10), the values $\Psi_1=\Psi(x_1)$ and $\Psi_2=\Psi(x_2)$ at any two positions x_1,x_2 can be interpreted as the surface potentials of a (fictive) pair of charged plates. Some arbitrary examples of such pairs of plates are indicated in Fig. 1 by the bold vertical lines. The surfaces of these plates are located in x_1 and x_2, they carry a charge density given by the derivative of Ψ in x_1 and x_2, and interact across the separation distance $L=|x_1-x_2|$ through the pressure P associated with the function $\Psi(x)$. Within the Poisson-Boltzmann approximation, two plates with an equal sign of charge can only repel each other [42] as in the example of Fig. 1(a).

Our previous observations suggest a simple way of calculating the separation distances between two (real) dissimilar charged surfaces for a given value of the pressure. We have noted that for every nonzero pressure P, the function $\Psi(x)$ satisfying the Poisson-Boltzmann equation [Eq. (1)] is symmetric or antisymmetric with respect to the origin, which can, but need not, lie between the surfaces.

The basic idea is to divide the system as illustrated in Fig. 2: we will consider the surfaces separately as if they were interacting, not with each other, but with the plane at $x=0$. For each surface, we calculate the pressure at all distances from that plane; then we combine *those* distances of both surfaces that belong to the same pressure P in order to obtain all the surface separations L at which this pressure is actually assumed by our system of dissimilar plates.

1. Boundary conditions

Clearly, the surface positions x_1 and x_2 compatible with a given pressure P will depend on the individual charging characteristics of each surface. These charging characteristics can be taken into account by an appropriate choice of boundary conditions for Eq. (1). For the sake of simplicity, it is rather common to consider either the electrostatic surface potential or the surface charge density as constant, and for some types of materials, these assumptions are legitimate. A condition of ''constant charge'' arises naturally, for instance, if the surface charge is due to the dissociation of very strongly acidic or basic surface headgroups, like in the example of sulfate latex discussed below.

In many practical situations, however, a more realistic description considers the chemical equilibrium of partially dissociated surface groups with the bulk electrolyte at all surface separations [16,19,36]. The implied requirement of constant chemical potential of the charge determining ion generally entails a nontrivial, material-specific relation

$$f_j(\Psi_j,\sigma_j)=0; \qquad \text{for} \quad j=1,2 \tag{11}$$

between the surface potential and the charge density of the surface j. This type of boundary condition usually leads to the simultaneous variation of the charge and surface potential with separation known as ''charge regulation'' [17,22]. Examples of charge-regulating surfaces will also be discussed below.

It will be useful to define an individual distance $D_j, j=1,2$ of the surface j from the origin, which has the same absolute value as the x coordinate at the position of the surface ($|D_j|=|x_j|$) but will be considered as negative if the surface j lies between the plane of origin and the second surface (see Fig. 2). On the other hand, if the plane of origin and the solution-filled gap between the two surfaces lie on the same side of the surface j, then D_j will be taken as positive. Formally, this can be expressed as

$$D_j=\begin{cases} -|x_j|, & \mathrm{sgn}(x_1/x_2)>0>|x_j|-|x_{3-j}| \\ |x_j|, & \text{else} \end{cases} \qquad j=1,2. \tag{12}$$

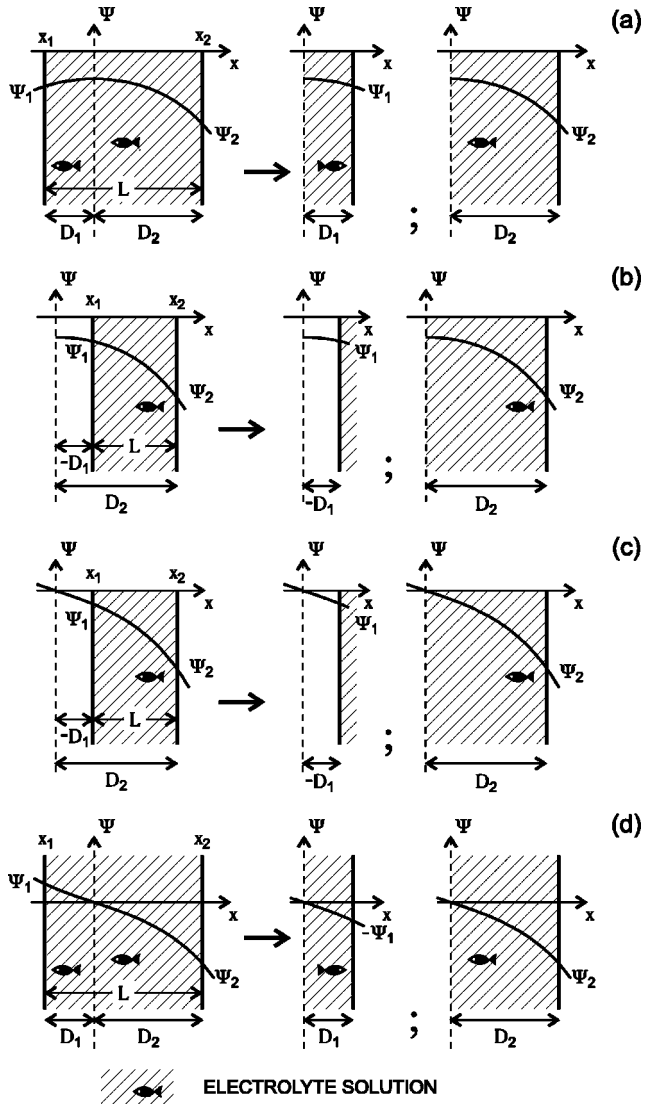

FIG. 2. The division into two subsystems of just one surface interacting with the plane of symmetry for the electrostatic potential $\Psi(x)$. The hatched area indicates the space filled by the electrolyte solution. In order for Eqs. (4)–(8) to be applicable, the potential must be considered in the fourth quadrant ($x>0$, $\Psi<0$). (a) The situation of two surfaces with equal sign of charge. In this case the interaction according to the Poisson-Boltzmann equation can only be repulsive. (b) Repelling surfaces with unequal sign of charge. The surface pointing away from the plane of symmetry is considered to have a negative distance from that plane. (c) Attracting surfaces with equal sign of the surface potential. (d) Attracting surfaces with unequal sign of the surface potential.

Whatever the precise form of the boundary condition, it can now be applied to the differential equation (1) by substituting

$$\Psi_j = \Psi(x = |D_j|) \tag{13}$$

and

$$\sigma_j = \mathrm{sgn}(D_j) \frac{\varepsilon \varepsilon_0 k_B T}{e_0 z} \left. \frac{d\Psi}{dx} \right|_{x=|D_j|}, \tag{14}$$

where the functions $\Psi(x)$ and $d\Psi/dx$ in Eqs. (13) and (14) are given by Eqs. (4) and (5) for repulsive interaction and by Eqs. (7) and (8) for attractive interaction. With the above substitutions, Eq. (11) is a single transcendental equation connecting either the pressure itself (attractive case) or the closely related potential extremum Ψ_0 (repulsion) to the individual distance D_j from the plane of origin. Solving this equation for all individual distances $-\infty < D_j < \infty$ thus leads to the function P_j of the pressure that the surface j experiences at any distance D_j.

2. Combining the two surfaces

Since at every configuration both surfaces must experience the same pressure, only those pressures P can be realized that satisfy

$$P = P_1(D_1) = P_2(D_2) \tag{15}$$

for some individual distances D_1 and D_2 (which, however, need not be unique). The corresponding surface separation L is then given by the sum of the individual distances

$$L(P) = D_1 + D_2, \tag{16}$$

with only positive separations L reflecting a real situation.

At large surface separations and correspondingly weak interaction, the surfaces are always situated on both sides of the plane of origin like in Figs. 2(a) or 2(d). Moreover, the situation is always like Fig. 2(a) as long as both surfaces have the same sign of charge. Two surfaces with unequal signs of charge at smaller separation may, however, be located on the same side of the plane of origin; this situation is sketched in Fig. 2(b) for a repulsive and in Fig. 2(c) for an attractive interaction. As the surfaces approach each other, one of them may actually ''cross'' the origin, i.e., the potential on this surface may change sign if the interaction at this separation is attractive, or the charge of this surface may be reversed if the interaction is repulsive.

By associating each pressure that can be realized for both surfaces individually with the corresponding surface separations, we obtain the complete force profile $P(L)$ for the system of dissimilar surfaces. The actual surface potentials and surface charge densities as a function of surface separation L follow from Eqs. (14) and (13) as the surface properties σ_j and Ψ_j associated with the individual distances D_j from the plane of origin.

III. EXAMPLES

As an illustration we apply the proposed method to two examples. First, we will consider a carboxyl latex surface and a sulfate latex surface interacting across a monovalent electrolyte at pH 4 and an ionic strength of 1 mM. As a second example, we will discuss the interaction between a silica surface and a rutile surface at the same ionic strength and pH 6.5. The sulfate groups will be considered as fully deprotonated at all times and the resulting surface charge as constant. All other materials will be described in the framework of a 1-pK-basic Stern Model [43,44]. Within this model (and for $z=1$), the boundary condition for a charge-regulating surface j reads [38]

TABLE I. Exemplary materials.

Material[a]	pK	$\Gamma_{tot}(nm^{-2})$[b]	$(\Gamma_{ref}/\Gamma_{tot})$[c]	$C^S(F/m^2)$[d]
Carboxyl latex	4.9	0.5	1	∞
Sulfate latex[e]		0.1		
Silica	7.5	8.00	1	2.9
Rutile	5.8	12.2	1/2	1.33

[a]The association of the tabulated properties with the individual surfaces of different materials is marked by the subscript j in Eq. (17)
[b]Total density of surface headgroups.
[c]Fraction of the total number of sites that are protonated in the zero charge configuration.
[d]Stern capacity.
[e]For this surface, a boundary condition of constant charge $\sigma = e_0\Gamma_{tot}$ has always been used.

$$\Psi_j = (\mathrm{pK}_j - \mathrm{pH})\ln 10 - \frac{e_0\sigma_j}{k_B T C_j^S} + \ln\frac{e_0(\Gamma_{tot,j} - \Gamma_{ref,j}) - \sigma_j}{e_0\Gamma_{ref,j} + \sigma_j}, \tag{17}$$

where the pK value refers to a single deprotonation reaction, C_j^S is the Stern capacity, $\Gamma_{tot,j}$ the total density of chargeable surface headgroups, and $\Gamma_{ref,j}$ the (reference) density of protonated headgroups at which the surface j is uncharged [38]. The parameters used are summarized in Table I.

A. Carboxyl latex — sulfate latex

Both latex surfaces can only be negatively charged, which implies that only repulsive interaction is possible, and that the plane of symmetry for the electrostatic potential $\Psi(x)$ always lies between the surfaces, thus only positive distances D_{Carboxyl} and D_{Sulfate} from this plane have to be considered. [In other words, the scenario shown in Fig. 2(a) applies at all separations.]

The resulting pressure as a function of the surface separation L is shown on the left hand side of Fig. 3(a), along with the corresponding curves for boundary conditions of constant charge (cc) or constant electrostatic potential (cp) on both surfaces. In the same representation, the left hand side of Figs. 3(b)–(e) shows the variation of the surface potentials and charge densities with separation.

The dividing pressure in this system is seen to increase monotonically with decreasing surface separation; at contact it diverges. The potential on both surfaces is negative and diverges for $L \to 0$ as well. The carboxylic surface loses its

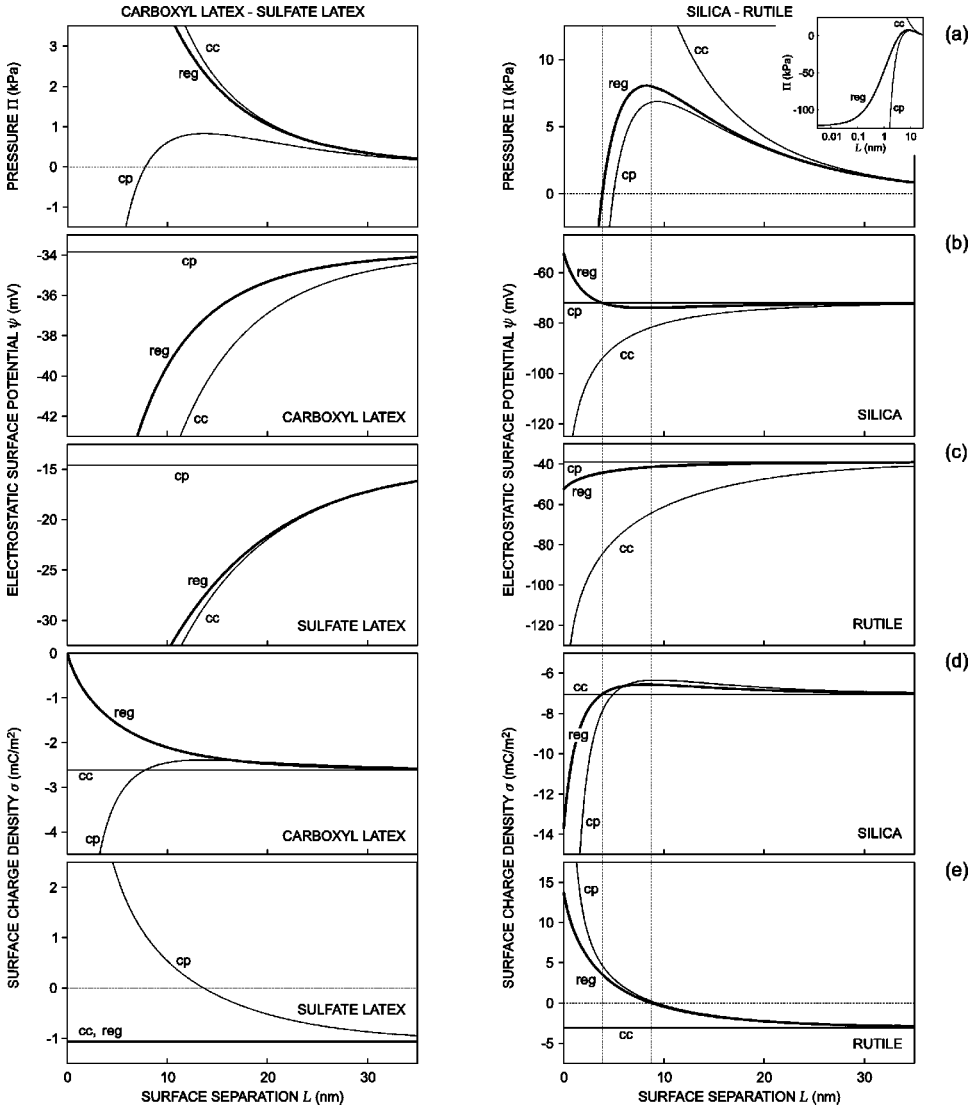

FIG. 3. The interaction between a carboxyl latex and a sulfate latex surface (left) at pH 4 and between a silica surface and a rutile surface (right) at pH 6.5. For both systems, an ionic strength of 1 mM (1-1-electrolyte, $\kappa^{-1} = 9.6$ nm) has been used. (a) The force per unit area for boundary conditions of charge regulation (reg), constant charge on both surfaces (cc), and constant electrostatic potential on both surfaces (cp). Inset: A semilogarithmic representation on a larger scale reveals qualitative differences between the silica-rutile interaction at constant potential and charge regulation. (b) and (c) The corresponding electrostatic surface potentials. (d) and (e) The surface charge densities. Broken vertical lines in the silica-rutile indicate the separation of zero force (3.8 nm) and the separation of charge reversal on the regulating rutile surface (8.8 nm). Above the latter separation the system resembles the one sketched in 2(a), for 3.8 nm$<L<$8.8 nm it looks like 2(b), at even smaller separations (left of both vertical lines), the situation looks like in 2(c).

charge in this limit, whereas the charge on the sulfate surface remains unchanged. Apart from the decharging of the carboxyl groups at small separations, this system of two dissimilar surfaces behaves in a rather similar way as the system where *both* surfaces are subject to boundary conditions of constant charge—even though carboxylic surfaces are known to regulate their charge rather well for the given parameters of the electrolyte solution [38].

If the potential on both surfaces is fixed, the behavior is very different. At large separations, it is qualitatively the same, but at a separation of 14 nm, the pressure and the charge on the carboxylic surface go through a maximum, while the charge on the sulfate surface goes through zero. At a separation of 7.8 nm the force is zero and the carboxylic surface resumes its charge of the large separation limit, because it does not feel the presence of the sulfate surface. At even shorter separations the force at constant potential is attractive; it diverges in the limit of contact.

B. Silica – rutile

The charge-regulating silica surface, like the latex surfaces, can only be negatively charged. The rutile surface on the other hand, though negatively charged in isolation at the chosen pH, can undergo a charge reversal, and therefore negative distances D_{Rutile} have to be considered as well. As it turns out, the system actually passes the situations sketched in Figs. 2(a), 2(b), and 2(c), in this order, as the two surfaces approach each other.

Results for the silica-rutile system are presented on right hand side of Fig. 3. At large separation, both surfaces behave qualitatively as they would in a perfectly symmetric system [38]: as they approach each other, a repulsive pressure and the absolute surface potentials are enhanced, whereas the absolute charge density is reduced. At a separation of 8.8 nm the rutile surface reaches its Nernst potential $(\mathrm{pK}-\mathrm{pH})(\ln 10)k_BT/e_0=41.4$ mV and undergoes a charge reversal. A maximum pressure of 8.0 kPa is reached at $L=8.2$ nm. Upon further approach the pressure drops again, passes zero at $L=3.8$ nm (at which point the silica surface resumes the surface properties of an isolated surface), and eventually reaches a finite contact value [of -121 kPa, see the inset of Fig. 3(a)]. The potential at contact is -52.4 mV for both surfaces, while the charge density goes to $+13.7$ mC/m^2 for the rutile surface and -13.7 mC/m^2 for the silica surface. This behavior is different from the one observed when both surfaces are subject to either constant charge or constant potential conditions. Under these simplified boundary conditions, no qualitative differences are resolved between the two different systems presented in Fig. 3: whether in the latex-latex system or in the silica-rutile example, both times the requirement of constant charge causes a monotonically increasing repulsion between approaching surfaces, and constant potential causes an electrostatic attraction at short separations. Also note that for the silica surface, the regulated surface potential curve crosses the constant potential curve, and the charge curves for different boundary conditions all have crossing points as well. In this sense, charge regulation in a system of dissimilar surfaces does not lead to an intermediate behavior between the cases of constant charge and constant potential as it does in systems of identical surfaces. Moreover, the regulation behavior of this system is rather similar, at most separations, to the case of constant potential, even though the silica surface would not behave like a constant potential surface when interacting with another silica surface, given the same parameters for the electrolyte [38].

Our discussion of the silica-rutile system only serves to illustrate the proposed computational technique, and we did not try to model any particular experiment. Nevertheless, it should be mentioned that the force between a SiO_2 sphere and a TiO_2 crystal has been measured under conditions comparable to the ones of Fig. 3. The experiment seems to indicate a rather more constant-charge-like behavior [8]. Since, however, the measured force does not only contain the pure electrostatic component but also dispersion forces and most likely an additional short-range repulsion, conclusions about the ''true regulation behavior'' must be drawn with caution.

IV. CONCLUSION

We have presented an exact method to calculate the double layer force between charge-regulating plates of dissimilar composition and charging behavior on the level of the (nonlinear) Poisson-Boltzmann theory. The proposed strategy is computationally straightforward and does not require a numerical solution of the differential equation.

We have applied this strategy to the exemplary case of a carboxylic latex surface and a sulfate latex surface as well as to the system of a silica and a rutile surface interacting across a monovalent electrolyte. The amphoteric behavior of the rutile gives rise to a rather complex force profile, including a transition from repulsion at large separations to attraction at short separations for a pH at which the *isolated* surfaces are both negatively charged. This behavior is very different from the interaction in systems of two identical surfaces. A description based on the assumption of constant charge or constant potential on both (dissimilarly charged) surfaces misses qualitative features of the true interaction profile under conditions of charge regulation.

ACKNOWLEDGMENTS

We would like to thank Hans Sticher for his support. This work was financed by the Swiss National Science Foundation and by the US National Science Foundation (Grant No. CTS-9820795).

APPENDIX

Equation (2) already states the result of a first integration of the Poisson-Boltzmann equation

$$\left(\frac{d\Psi}{dx}\right)^2=2\kappa^2\cosh\Psi-\kappa^2(P+2). \tag{A1}$$

Expressed in terms of

$$\Omega(x)=\exp[\Psi(x)-\Psi_0] \tag{A2}$$

and

$$\xi=\exp(\Psi_0), \tag{A3}$$

Eq. (A1) reads

$$\left(\frac{1}{\Omega}\frac{d\Omega}{dx}\right)^2=\kappa^2\left[\xi\Omega+\frac{1}{\xi\Omega}-(P+2)\right]. \tag{A4}$$

For $\Psi\leqslant 0$ and $x\geqslant 0$, $d\Omega/dx$ is negative, and separation of variables leads to

$$\int_1^{\Omega}\frac{d\Omega'}{\sqrt{\Omega'[\xi^2\Omega'^2-(P+2)\xi\Omega'+1]}}=-\frac{\kappa x}{\sqrt{\xi}}. \tag{A5}$$

Further manipulation of the elliptic integral on the left hand side of Eq. (A5) is greatly facilitated by using the properties of the so-called Jacobian elliptic functions [40]. The functions $\mathrm{sn}(u|m)$, $\mathrm{cn}(u|m)$, and $\mathrm{dn}(u|m)$ of argument u and parameter m $(0\leqslant m\leqslant 1)$ are defined as the inverse of the following integrals:

$$u=\int_0^{\mathrm{sn}(u|m)}\frac{dt}{\sqrt{(1-t^2)(1-mt^2)}}, \tag{A6}$$

$$u=\int_1^{\mathrm{cn}(u|m)}\frac{dt}{\sqrt{(1-t^2)(1-m+mt^2)}}, \tag{A7}$$

$$u=\int_1^{\mathrm{dn}(u|m)}\frac{dt}{\sqrt{(1-t^2)(t^2-1+m)}}. \tag{A8}$$

Further elliptic functions are defined as

$$\mathrm{cd}(u|m)=\mathrm{cn}(u|m)/\mathrm{dn}(u|m) \tag{A9}$$

and

$$\mathrm{sd}(u|m)=\mathrm{sn}(u|m)/\mathrm{dn}(u|m). \tag{A10}$$

We will make use of their periodicity properties

$$\mathrm{sn}(K(m)-u|m)=\mathrm{cd}(u|m) \tag{A11}$$

and

$$\mathrm{cn}(u-K(m)|m)=\sqrt{1-m}\,\mathrm{sd}(u|m), \tag{A12}$$

where

$$K(m)=\int_0^1\frac{dt}{\sqrt{(1-t^2)(1-mt^2)}}=\int_0^1\frac{dt}{\sqrt{(1-t^2)(1-m+mt^2)}} \tag{A13}$$

is the quarter period of the elliptic functions along the real axis, also called the complete elliptic integral of the first kind [40].

The derivatives of the elliptic functions needed to deduce the the expressions for $d\Psi/dx$ in Eqs. (5) and (8) are

$$\frac{d}{du}\mathrm{sn}(u|m)=\mathrm{cn}(u|m)\,\mathrm{dn}(u|m), \tag{A14}$$

$$\frac{d}{du}\mathrm{cn}(u|m)=-\mathrm{sn}(u|m)\,\mathrm{dn}(u|m), \tag{A15}$$

$$\frac{d}{du}\mathrm{dn}(u|m)=-m\,\mathrm{sn}(u|m)\,\mathrm{cn}(u|m). \tag{A16}$$

1. Repulsive case ($P>0$)

According to Eqs. (2) and (A3) positive pressures can be expressed as

$$P=\xi+1/\xi-2. \tag{A17}$$

Inserting Eq. (A17) into Eq. (A5) yields

$$\begin{aligned}\frac{\kappa x}{\sqrt{\xi}}&=-\int_1^{\Omega}\frac{d\Omega'}{\sqrt{\Omega'(1-\Omega')(1-\xi^2\Omega')}}\\&=-\int_1^{\sqrt{\Omega}}\frac{2dt}{\sqrt{(1-t^2)(1-\xi^2t^2)}}\end{aligned} \tag{A18}$$

or

$$\begin{aligned}\frac{\kappa x}{2\sqrt{\xi}}=u&=-\int_1^0\frac{dt}{\sqrt{(1-t^2)(1-\xi^2t^2)}}\\&\quad-\int_0^{\sqrt{\Omega}(x)}\frac{dt}{\sqrt{(1-t^2)(1-\xi^2t^2)}}\\&=K(\xi^2)-\mathrm{sn}^{-1}(\sqrt{\Omega}),\end{aligned} \tag{A19}$$

where the last equality uses the defining Eqs. (A13) and (A6), and sn^{-1} denotes the inverse function of $\mathrm{sn}(u|m)$. According to Eq. (A11)

$$\Omega(x)=\mathrm{sn}^2(K(\xi^2)-u|\xi^2)=\mathrm{cd}^2(u|\xi^2), \tag{A20}$$

which is the result cited in Eq. (4).

2. Attractive case ($P<0$)

In the attractive case $\xi=1$, and with the substitution

$$\omega=\frac{1-\Omega}{1+\Omega}, \tag{A21}$$

Eq. (A5) takes the form

$$\kappa x=\int_0^{\omega}\frac{d\omega'}{\sqrt{(1-\omega'^2)[-P/4+(1+P/4)\omega'^2]}}. \tag{A22}$$

If $-1\leqslant P/4\leqslant 0$, then after splitting the integration domain in Eq. (A22),

$$\int_0^{\omega}f(\omega')\,d\omega'=\int_0^1 f(\omega')\,d\omega'+\int_1^{\omega}f(\omega')\,d\omega', \tag{A23}$$

Eqs. (A13) and (A7) can be applied to give

$$\kappa x=K(1+P/4)+\mathrm{cn}^{-1}(\omega|1+P/4), \tag{A24}$$

and according to Eq. (A12)

$$\omega=\sqrt{-P/4}\,\mathrm{sd}(\kappa x|1+P/4). \tag{A25}$$

If, on the other hand, $P/4 \leqslant -1$, then after multiplication of Eq. (A22) by $\sqrt{-P/4}$, it follows from Eq. (A6) that

$$\omega = \mathrm{sn}[\tfrac{1}{2}(-P)^{1/2}\kappa x | 1+4/P]. \tag{A26}$$

Equstions (A25) and (A26) are the results cited in Eq. (7).

3. Limits of parameter values

Equations. (A19) and (A24) imply that

$$0 \leqslant \frac{\kappa x}{2\sqrt{\xi}} \leqslant K(\xi^2) \quad \text{for} \quad P>0 \tag{A27}$$

and

$$0 \leqslant \kappa x \leqslant K(1+P/4) \quad \text{for} \quad -4<P<0, \tag{A28}$$

which, in principle, limits the range of x for which the derived expressions for $\Psi(x)$ are valid. The quarter period, however, diverges in the limit of zero pressure (then the parameter m goes to 1); therefore, at large surface separations, when $\Psi(x)$ must be evaluated at large x, the given formulas are also valid for a large range of x. We found that the above mentioned conditions [Eqs. (A27) and (A28)] were satisfied automatically for all positions x relevant in this study.

4. The linearized case

When the electrostatic potential is small [i.e., $|\Psi(x)| \leqslant 1$ between the surfaces] then Eq. (1) can be linearized, and the solution of the Debye Hückel equation,

$$\frac{d^2\Psi}{dx^2} - \kappa^2\Psi = 0, \tag{A29}$$

corresponding to Eqs. (4), (7), and (9) reads

$$\Psi(x) = \begin{cases} -\operatorname{arccosh}(1+P/2)\cosh\kappa x, & P>0 \\ -|P|^{1/2}\sinh\kappa x, & P<0 \\ \Psi_1 e^{-\kappa(x-x_1)}, & P=0. \end{cases} \tag{A30}$$

5. Superposition

If $P \neq 0$ and $|\kappa x_1|, |\kappa x_2| \gg 1$, then Eq. (A30) is well approximated by the linear superposition result

$$\Psi(x) = \begin{cases} -2|\Psi_j^\infty| e^{-\kappa|x_j|}\cosh\kappa x, & P>0 \\ -2|\Psi_j^\infty| e^{-\kappa|x_j|}\sinh\kappa x, & P<0, \end{cases} \tag{A31}$$

where Ψ_j^∞, $j=$ 1 or 2, is the potential of either one of the surfaces in isolation. If these surface potentials are too high for Eq. (1) to be linearized ($\Psi_j^\infty \geqslant 1$), then Eq. (A31) will still be a good approximation for small x (but large x_1, x_2) when the surface potential is replaced by the ''effective potential''

$$\Psi_j^\infty \rightarrow \Psi_{j,\mathrm{eff}}^\infty = 4\tanh(\Psi_j^\infty/4), \tag{A32}$$

which in the linear theory yields the same potential decay far away from the isolated surface as the true, ''bare'' potential does in the nonlinear treatment [Eq. (9)] [12]. Obviously, $\Psi_{j,\mathrm{eff}}^\infty \rightarrow 4$ in the limit of high bare potentials Ψ_j^∞ and the corresponding effective charge density saturates for high bare charge σ_j to the value $\sigma_{\mathrm{eff}} \rightarrow 4\varepsilon\varepsilon_0\kappa k_B T/e_0$, known as the condensation limit [45,46].

[1] J. Israelachvili, *Intermolecular & Surface Forces*, 2nd ed. (Academic Press, London, 1991).
[2] J. Israelachvili, J. Chem. Soc., Faraday Trans. 1 **74**, 975 (1978).
[3] R.M. Pashley, J. Colloid Interface Sci. **83**, 531 (1981).
[4] J. Israelachvili and R.M. Pashley, Nature (London) **306**, 249 (1983).
[5] R.G. Horn, D.R. Clarke, and M.T. Clarkson, J. Mater. Res. **3**, 413 (1988).
[6] G. Binnig, C. Quate, and G. Gerber, Phys. Rev. Lett. **56**, 930 (1986).
[7] H.-J. Butt, M. Jaschke, and W. Ducker, Biochem. Bioenerg. **38**, 191 (1995).
[8] I. Larson, C.J. Drummond, D.Y.C. Chan, and F. Grieser, J. Phys. Chem. **99**, 2114 (1995).
[9] G. Toikka, R.A. Hayes, and J. Ralston, J. Chem. Soc., Faraday Trans. **93**, 3523 (1997).
[10] I. Larson, C.J. Drummond, D.Y.C. Chan, and F. Grieser, Langmuir **13**, 2109 (1997).
[11] P. Hartley, I. Larson, and P.J. Scales, Langmuir **13**, 2207 (1997).
[12] W. B. Russel, D. A. Saville, and W. R. Schowalter, *Colloidal Dispersions* (Cambridge University Press, Cambridge, 1989).
[13] B.V. Derjaguin and L. Landau, Acta Physicochim. URSS. **14**, 633 (1941).
[14] E. J. W. Verwey and J. Th. G. Overbeek, *Theory of the Stability of Lyophobic Colloids* (Elsevier, Amsterdam, 1948).
[15] L. Guldbrand, B. Jönsson, H. Wennerström, and P. Linse, J. Phys. Chem. **80**, 2221 (1984).
[16] B.W. Ninham and V.A. Parsegian, J. Theor. Biol. **31**, 405 (1971).
[17] D.Y.C. Chan, J.W. Perram, L.R. White, and T.W. Healy, J. Chem. Soc., Faraday Trans. 1 **71**, 1046 (1975).
[18] D.Y.C. Chan, T.W. Healy, and L.R. White, J. Chem. Soc., Faraday Trans. 1 **72**, 2844 (1976).
[19] D.C. Prieve and E. Ruckenstein, J. Theor. Biol. **56**, 205 (1976).
[20] D.C. Prieve and E. Ruckenstein, J. Colloid Interface Sci. **60**, 337 (1977).
[21] D.C. Prieve and E. Ruckenstein, J. Colloid Interface Sci. **63**, 317 (1978).
[22] T.W. Healy, D. Chan, and L.R. White, Pure Appl. Chem. **52**, 1207 (1980).
[23] G.M. Bell and G.C. Peterson, Can. J. Chem. **59**, 1888 (1981).

[24] D.Y.C. Chan and D.J. Mitchell, J. Colloid Interface Sci. **95**, 193 (1983).
[25] D. Y. C. Chan, in *Geochemical Processes at Mineral Surfaces*, edited by J. A. Davis and K. F. Hayes, *ACS Symposium Series* (American Chemical Society, Washington, DC, 1986) Vol. 323, p. 99.
[26] I.M. Metcalfe and T.W. Healy, Faraday Discuss. Chem. Soc. **90**, 335 (1990).
[27] J.W. Krozel and D.A. Saville, J. Colloid Interface Sci. **150**, 365 (1992).
[28] S.L. Carnie and D.Y.C. Chan, J. Colloid Interface Sci. **155**, 297 (1993).
[29] S.L. Carnie and D.Y.C. Chan, J. Colloid Interface Sci. **161**, 260 (1993).
[30] A. Grabbe, Langmuir **9**, 797 (1993).
[31] E.S. Reiner and C.J. Radke, Adv. Colloid Interface Sci. **47**, 59 (1993).
[32] S.L. Carnie, D.Y.C. Chan, and J.S. Gunning, Langmuir **9**, 797 (1993).
[33] D. McCormack, S.L. Carnie, and D.Y.C. Chan, J. Colloid Interface Sci. **169**, 177 (1995).
[34] J. Stankovich and S.L. Carnie, Langmuir **12**, 1453 (1996).
[35] J.P. Hsu and Y.C. Kuo, J. Colloid Interface Sci. **183**, 194 (1996).
[36] J. Stahlberg and B. Jönsson, Anal. Chem. **68**, 1536 (1996).
[37] N.S. Pujar and A.L. Zydney, J. Colloid Interface Sci. **192**, 338 (1997).
[38] S.H. Behrens and M. Borkovec, J. Phys. Chem. B **103**, 2918 (1999).
[39] The following analysis can, in principle, be extended to cover systems with asymmetric electrolytes. However, such an extension might be of doubtful value, since for those systems the neglect of ion correlations leads to a much poorer description of the true electrostatic potential, see J. Uhlander and R. Kjellander, J. Chem. Phys. **109**, 9508 (1998).
[40] M. Abramowitz and A. Stegun, *Handbook of Mathematical Functions*, 9th ed. (Dover Publications, New York, 1972); I. S. Gradshteyn and I. M. Ryzhik *Table of Integrals, Series, and Products* Academic Press, San Diego, 1979 (Corrected and enlarged edition).
[41] Calculations presented below used the *NAG Fortan Library* 1st ed. (Mark 16) (NAG Ltd., Oxford, 1993).
[42] The correlation between counterions can lead to a net attraction even between surfaces with equal signs of charge, see, e.g., I. Rouzina and V.A. Bloomfield, J. Phys. Chem. **100**, 9977 (1996); N. Grønbech-Jensen, R.J. Mashl, R.F. Bruinsma, and W.M. Gelbart, Phys. Rev. Lett. **78**, 2477 (1997), and references therein. On the Poisson-Boltzmann level of approximation, this effect cannot be resolved.
[43] T.W. Healy and L.R. White, Adv. Colloid Interface Sci. **9**, 303 (1978).
[44] J. Westall and H. Hohl, Adv. Colloid Interface Sci. **12**, 265 (1980).
[45] S. Alexander, P.M. Chaikin, P. Grant, G.J. Morales, P. Pincus, and D. Hone, J. Chem. Phys. **80**, 5776 (1984).
[46] T. Gisler, S.F. Schulz, M. Borkovec, H. Sticher, P. Schurtenberger, B. D'Aguanno, and R. Klein, J. Chem. Phys. **101**, 9924 (1994).